Proceedings World Geothermal Congress 2026
Calgary, Canada, June 8 – 11, 2026

Conceptual Model of the Ijen Geothermal Field, East Java: Indonesia's First Developed Blind Geothermal System

Ryan Libbey[1]*, Isto Saputra[2], John Murphy[1], Munazyi Husein[2], Fikri Dermawan[1], Dalmathias Archady[1], Rizal Abiyudo[2], Simon Webbison[1], Novianto[2], Ando Deuhart[2], Darren Utomo[2], Adam Johnson[1], Paul Spielman[1], Beta Kurniawahidayati[1], Zach Reynolds[1], Julfi Hadi[2], William Cumming[3], Luigi Marini[4], Mauro Parini[5], Alfend Rudyawan[6], Irene Wallis[7], and Idham Andri Kurniawan[6]

Ormat Technologies Inc.[1]*, P.T. Medco Cahaya Geothermal[2] (presently or formerly), Cumming Geoscience[3], STEAM srl[4], Independent Consultant[5], Institut Teknologi Bandung[6], Cubic Earth[7]

rlibbey@ormat.com

Keywords: Conceptual Model; Blind System; Exploration

ABSTRACT

The Ijen geothermal field is a high-enthalpy, caldera-hosted system in East Java. The system is liquid-dominated with a two-phase region extending from +200 to +750 mRSL. The ~1.5 km^2 upflow of the system is characterized by a >300°C, neutral pH, ~0.3 wt% TDS Na-Cl fluid, with ~0.15-0.3 wt% dissolved NCG in the deep reservoir. The resource is situated within the southern regions of the Pleistocene Kendeng Caldera, in the vicinity of numerous intracaldera volcanic features. One such feature, the Kawah Wurung maar, is adjacent to the upflow at Ijen and is interpreted to be a source of pronounced recharge into the system – resulting in steep lateral thermal gradients between wells. The resource area is devoid of active or fossil surface manifestations despite the occurrence of a relatively shallow boiling >300°C resource. This absence of surface features is the result of a deep (250-300 m) water table and the scrubbing of upward migrating steam and gas by shallow groundwater aquifers that flow laterally across the top of the argillic alteration zone. A sequence of competent and relatively unfractured Holocene lavas in the shallow stratigraphy at Ijen may also influence the lack of manifestations. The exploration and development drilling campaigns conducted by the Medco-Ormat joint venture in 2020-2024 achieved industry-leading results, with 9 of the 10 well legs exceeding their production/injection success thresholds. The conceptual model-driven approach to exploration implemented at Ijen was a key factor in achieving this success. The 34.5 MW Ormat two-phase binary plant at Ijen began commercial operations in February 2025.

1 INTRODUCTION

1.1 Project Location, Access, and Climate

The Ijen geothermal field is located in the province of East Java, Indonesia, 27 km from the city of Banyuwangi, which also represents the location of the nearest airport. The system is located 8 km to the west of, and is geologically distinct from, the Kawah Ijen volcanic system; a site consisting of a hyperacidic crater lake, superheated fumaroles (>400°C; Scher et al. 2013), and on-going traditional sulfur mining practices. The project is situated at an elevation range between 1500-1600 mRSL, with an average annual air temperature of 18.5°C.

1.2 Project History

Exploration of the Ijen geothermal prospect was initiated by Pertamina in the 1980-90s with 3G exploration and the drilling of the 690 m-deep ISH-01 slim hole. New 3G datasets were collected by ELC, NewQuest, Medco/Aboitiz in the 2010s and a slim hole campaign was conducted between 2016-2017. IJN-01 was completed to the intended depth (2000 m), however the second well of the campaign, IJN-02, was terminated early (775 m) for budgetary reasons. Ormat joined Medco as a JV partner in 2019 and began work on collecting new datasets and revising the conceptual model for the system. An exploration drilling campaign consisting of four deviated well legs was conducted in 2020-2021 (IJN6-1ST, IJN5-1, IJN6-2, and IJN6-1ST2). The results from this campaign justified a development drilling campaign undertaken in 2023-2024 that consisted of six wells (IJN2-1, IJN6-3, IJN6-4, IJN8-1, IJN8-2, and IJN9-1). The implementation of lessons-learned resulted in pronounced improvements of the days versus depth curves throughout the drilling campaigns. Overall, the campaigns executed by the Medco-Ormat joint venture achieved industry-leading results, with 9 of the 10 well legs exceeding their defined production/injection success thresholds. The conceptual model-driven approach to exploration implemented at Ijen was a key factor in achieving this success. The 34.5 MW Ormat two-phase binary plant at Ijen began commercial operations in February 2025, representing a fast project development timeframe of 4.8 years from the commencement of the Ormat-Medco exploration drilling program.

2 GEOLOGY AND GEOPHYSICS

2.1 Regional Geology and Tectonic Setting

Volcanism in Java is related to the NNE-directed subduction of the Indo-Australian plate beneath the Eurasian Plate, which has occurred along the Java trench beginning in the middle Eocene (Hall, 2002). The ~15 km-wide Kendeng Caldera (a.k.a. "Old Ijen Caldera") is a part of the Quaternary-modern volcanic arc, and formed as a result of the eruption and collapse of the Pleistocene Old Kendeng stratovolcano (a.k.a. "Old Ijen Volcano"; Sitorus, 1990) sometime between 300 ka (youngest pre-caldera deposit) to 50 ka (oldest post-caldera unit; the Mt. Blau lava flow). Six prominent composite cone volcanoes occur along the southern rim of the caldera, including (counterclockwise from east to west) Mt. Ringghi, Mt. Pawenen, Mt. Merapi, Mt. Rante, Mt. Jampit, and Mt. Suket. 13 intracaldera cones (basaltic andesite to dacite; Handley et al., 2007) occur in the southern half of the Kendeng Caldera, with ages ranging from 25 ka to recent.

NE-striking left-lateral faults are a repeating structural grain in Java and may relate to reactivated basement structures formed during the Late Cretaceous docking of the East Java-West Sulawesi (EJWS) microcontinental block with Sundaland, forming the Meratus Suture (Hall, 2012). Another structural fabric in Java, trending WNW-ESE, may be related to inherited extensional structures of the EJWS block. These latter features also manifest as conspicuous basement offsets in NW Australia, where the EJWS microcontinental block is modeled to have rifted from in the Late Jurassic (Hall et al., 2009, 2011, 2012; Figure 1). As discussed further below, both of these regional-scale structural fabrics are inferred to influence the location and permeability at Ijen.

A regional-scale NE-striking left-lateral strike-slip fault system is hypothesized to make a left-step at the location of the Kendeng Caldera; from the Gumitir Fault that is exposed in outcrop 25 km to the southwest of the Kendeng Caldera, to the Ringghi-Baluran Fault, which is inferred from prominent lineaments and volcano morphology/alignment (Marliyani et al., 2020; Figure 1). The step of this regional fault system creates a domain of inferred transtension/extension and related intracaldera volcanism in the south half of the caldera and it also equates to a local stress regime that is favorable for facilitating fluid flow along dilated fractures. The Ijen geothermal system, which occurs adjacent to multiple young intracaldera cones/craters in the southern region of the Kendeng Caldera, is an expression of this hydrothermal convection (Figure 1).

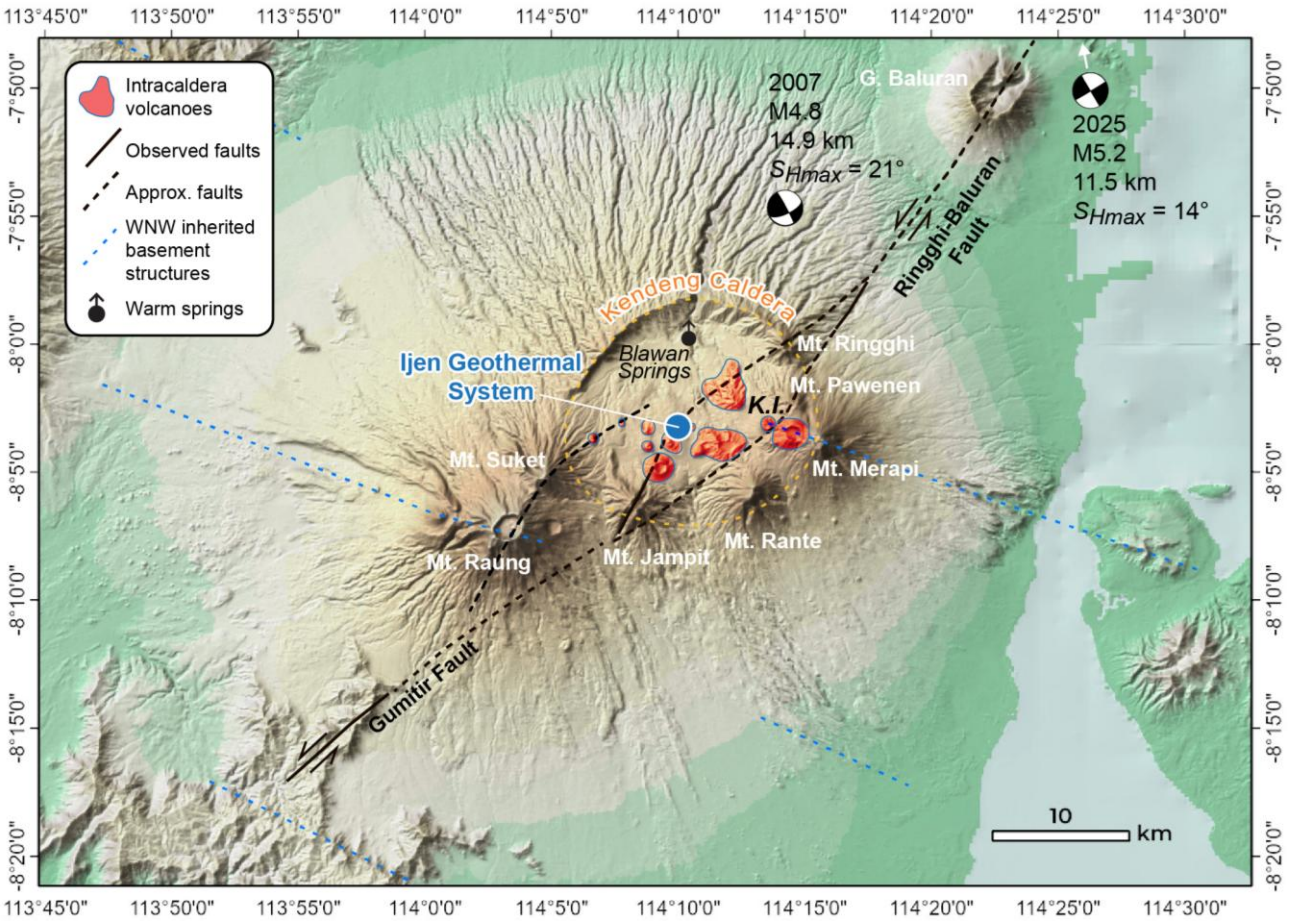


Figure 1. Regional structural setting hypothesized for the Ijen geothermal system. K.I. = Kawah Ijen Crater. Moment tensors from the USGS Earthquake Hazards Program and Ekström et al. (2012).

2.2 Local Geology and Structure

The stratigraphy of the Ijen geothermal system can be grouped into three temporal categories, corresponding to units that are pre-, syn-, and post-formation of the ~15 km-diameter Kendeng Caldera (Sujanto, 1988; Figure 2B). The caldera forming eruption resulted in the creation of the Kendeng Ignimbrite and the down-dropping of the basement Miocene sediments and Old Kendeng Volcano lithologies. A lake filled this depression until emptying ~50 ka through a fault system in the northern caldera wall (Caudron et al., 2015). Intracaldera monogenetic volcanoes occur directly within and around the Ijen geothermal field, including the Holocene maar/scoria cone complex of the Genteng Unit (Kawah Wurung), which may constitute a pronounced pathway of marginal recharge into the system. Lithologies directly relevant to the Ijen geothermal system are listed in Figure 2B and a cross-section of the geologic model is provided in Figure 8. A 3D geological model was constructed for Ijen based on data from surface mapping, cuttings analysis (including petrography/XRD), and electrofacies identification from image log data.

All of the listed units in Figure 2B have been intersected in wells at Ijen, except the basement Miocene sediments. The thickness of the Old Kendeng Volcano unit (>500-1000 m) is inferred based on the intersected thickness in wells at Ijen and from outcrop of this unit and the basement sediments on the northern regions/wall of the Kendeng Caldera. In addition to the above stratigraphy, a microdioritic intrusion (Figures 4A and 8) has been encountered in the bottom 500-800 mMD of wells IJN6-4 and IJN8-1, which appear to drill into the southern margins of the reservoir. A shorter interval of microdiorite was also intersected in the bottom 100-200 mMD of IJN6-2 and IJN6-1ST2. This microdiorite cross-cuts the Kendeng Ignimbrite and may be associated to Holocene intracaldera volcanism around Ijen.

Faults and fractures deduced from surface mapping, high-resolution DTM analysis, geophysical data, and wellbore image log analysis suggest a complex structural environment at Ijen. NE-, WNW-, and NW-striking faults occur within the field area, with the WNW-striking Geleman and Pandean Faults seemingly playing an important role in controlling the upflow location and geometry (Figure 2A). Elevated fracture density in the upflow location may result from the interaction of these WNW-structures with the (horse-tailing?) termination of the NE-striking Jampit Fault.

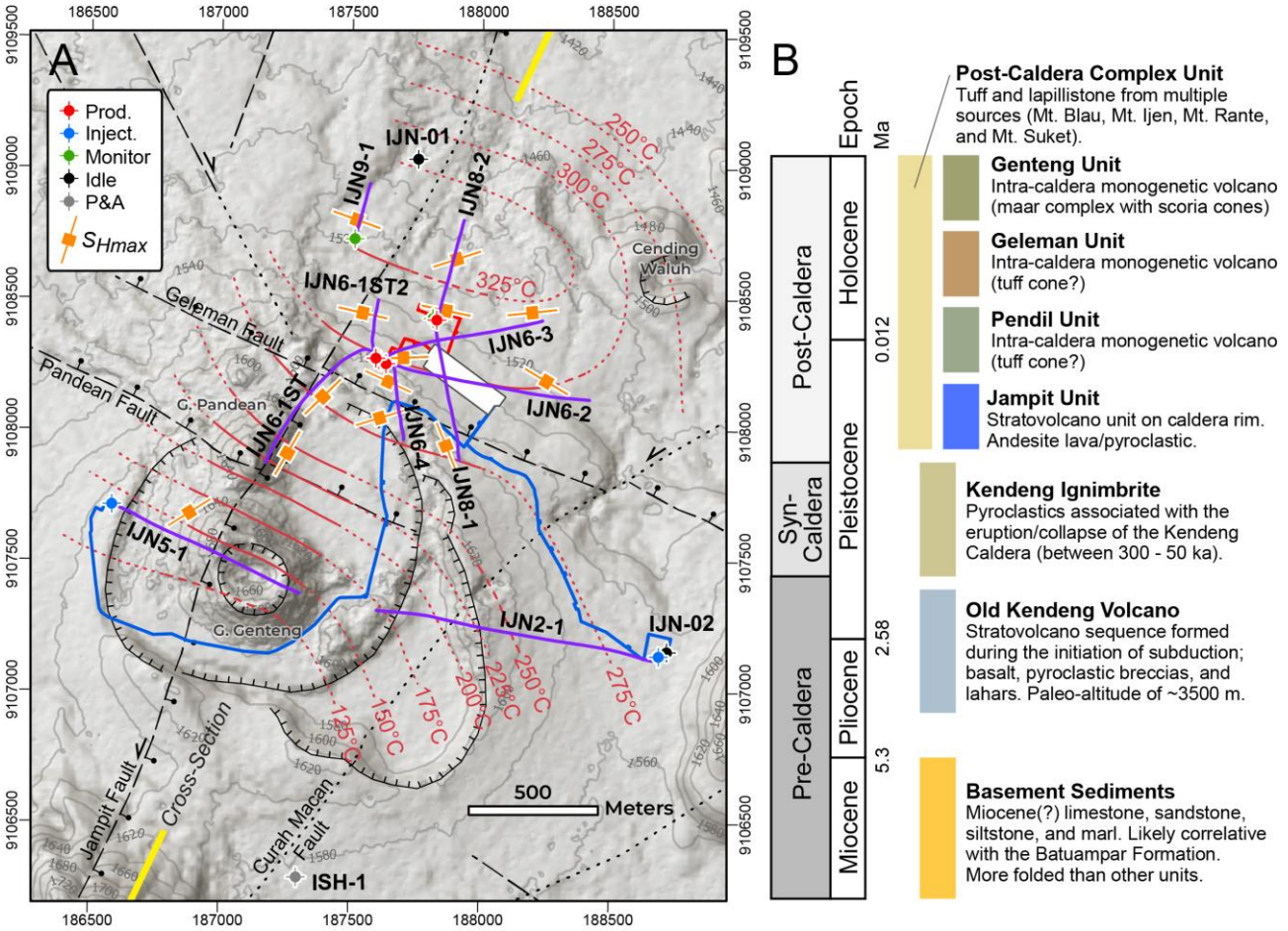


Figure 2. (A) Map of the Ijen Geothermal Field with faults and isotherms at -250 mRSL (dashed = higher confidence, dotted = lower confidence). Purple lines = well traces. (B) Stratigraphic column for Ijen.

2.3 Geomechanical Models and Stress Regime Systematics

Microresistivity image logs (utilizing the Haliburton XRMI tool and the Schlumberger FMI and FMS tools) were collected in all full-size wells, except IJN2-1. These data have been valuable for understanding permeability controls, volcanic stratigraphy, and stress field variation in the system. Interpretation of drilling-induced tensile fractures (DITF), and subsequent modelling to account for wellbore deviation, revealed that the dominant azimuth of the maximum horizontal stress direction (S_{Hmax}) varies from south to north (Figure 2A). In the south (IJN5-1, IJN6-1ST, and the deeper section of IJN6-4), it is broadly NE↔SW (with some deviation to the ENE and NNE), which is consistent with the regional intra-arc stress regime in Eastern Java (Figure 1). In contrast, northern wells (IJN9-1, IJN6-1ST2, IJN6-3, IJN6-2, and the upper sections of IJN8-2 and IJN6-4) revealed that the S_{Hmax} azimuth is broadly WNW↔ESE (with some deviation to E↔W). This rotation may be related to active faulting (e.g., Siler 2023), with the WNW-striking Geleman and Pandean Faults (perhaps with additional unmapped parallel structures) the most likely candidates. Borehole images also revealed more localized S_{Hmax} rotations that are interpreted to be coincident with faults intersected by the wells. Modelling found that wide, electrically conductive (possibly open) fractures had a higher slip and dilatation tendency in strike slip tectonics than normal conditions (Ferrill et al., 2020). This, combined with the dominance of high-angle fractures at reservoir depths, indicate that the local crustal regime is likely to be strike slip (or transitional) – in agreement with recent earthquake moment tensors and the hypothesized step-over structural setting for Ijen (Figure 1).

2.4 Hydrothermal Alteration Systematics

Rock cuttings from wells at Ijen were studied by binocular microscope, thin section petrography, XRD, and methylene blue analyses to estimate the bulk rock percentage of swelling clay (Gunderson et al., 2000). These studies reveal a well-developed prograding hydrothermal mineral sequence from argillic, to phyllic, to propyllitic assemblages with increasing depth at Ijen.

The argillic zone extends from approximately 100-750 mVD in the central parts of the field, and is characterized by common to abundant smectite, mixed-layer clay, and calcite. The contoured base of this zone correlates closely with the <3 ohm-m volume of the 3D MT inversion model for the field. The phyllic zone at Ijen is typically 350-450 m thick and is characterized by the occurrence of illite, increasing amounts of quartz, and spotty occurrences of trace anhedral epidote (i.e., “incipient epidote”; Ramos, 2002). The transition to the underlying propylitic zone is marked by the consistent occurrence of epidote. The propylitic zone generally corresponds to resistivity values of >10 ohm-m in the 3D MT inversion model. There is a deepening of the alteration zone boundaries, and corresponding conductor in the MT model, to the north of the production field, in the vicinity of IJN-01. This deepening trend relates to the NNE-dipping upflow geometry at Ijen, as discussed further below.

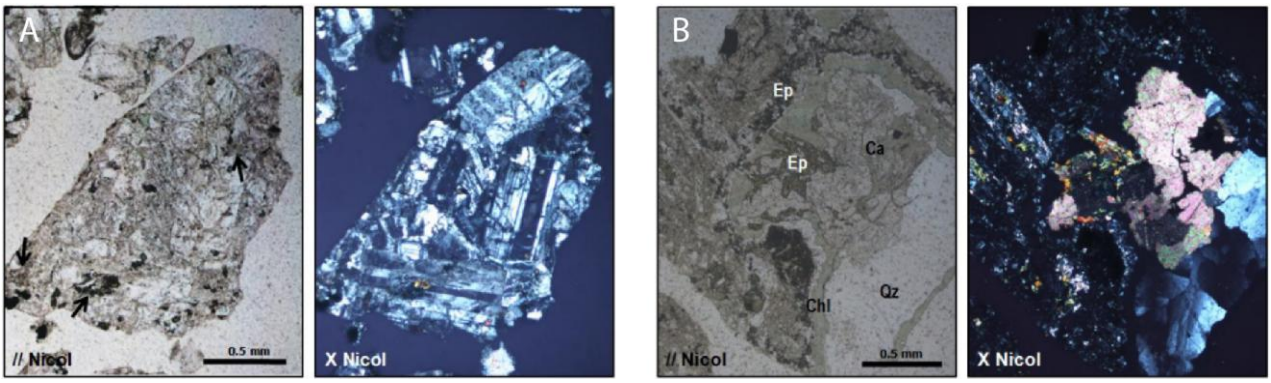


Figure 3. Photomicrographs from Ijen well cuttings. (A) Microdiorite in IJN6-4, 2094 mMD. (B) Resorbed epidote (Ep) being replaced by chlorite (Chl) and calcite (Ca) in IJN5-1, 1464 mMD.

Actinolite, a mineral generally considered to form at temperatures >300°C (Bird et al., 1984), is present in IJN8-1 from 1983 mMD to the TD of the well at 2800 mMD, although trace occurrences may also occur in two samples in IJN9-1 and IJN5-1. This interval in IJN8-1 corresponds to a dioritic intrusion, and it is likely that the occurrence of actinolite in this interval is related to elevated temperatures associated with this young intrusive body.

Pyrite and anhydrite are documented in all wells from Ijen, and occur over a wide elevation range from +1200 mRSL to the deepest drilled regions in the reservoir at approximately -1250 mRSL. There appears to be a general increase in anhydrite abundance in the eastern and southeastern regions of the field (i.e., IJN2-1, IJN8-1, IJN6-2, IJN6-3, IJN6-4, and IJN8-2) relative to the western and northwestern region of the field (e.g., IJN5-1, IJN6-1ST, and IJN9-1). The controls of the distribution pattern of anhydrite at Ijen is not well understood, but there may be a relationship to the hydrology of SO_4-rich marginal recharge fluids discussed in Section 3.

Notable disequilibrium is apparent when considering the temperature stability range of hydrothermal minerals in relation to the present-day subsurface temperatures at Ijen. For instance, elevated bulk-rock smectite concentrations (as determined by methylene blue analyses) are present in the Pad 6 wells at present-day measured temperatures of 250-280°C, far above the inferred upper-limit of 220°C for the transition of mixed-layer illite-smectite to end-member illite (Browne, 1984). The relationship suggests a geologically-recent heating trend in this part of the subsurface.

Conversely, propyllitic minerals such as epidote are present at elevations of +240 to -460 mRSL in IJN5-1, in the southwest region of the wellfield where subsurface temperatures are currently 125-175°C. Since epidote typically forms at minimum temperatures of 200-250°C in geothermal systems (Bird et al., 1984; Browne, 1984), the occurrences of this mineral in IJN5-1 suggest a pronounced cooling of this southwest region of the Ijen geothermal system. Regressive evolution of disequilibrium hydrothermal mineralogy is apparent in some occurrences of epidote from IJN5-1 that display resorbed textures and replacement by a lower temperature assemblage of chlorite and calcite (Figure 3B). The presence of actinolite in sections of IJN8-1 where the current subsurface temperature is interpreted to be ~275°C also supports the notion of a deep cooling trend in the southern part of the field.

3 GEOCHEMISTRY

A detailed summary of the liquid and gas chemistry of the Ijen geothermal system is provided by Dermawan et al. (2025), which characterizes the grouping of well chemistry at Ijen into four groups: the *Main Reservoir*, the *Upflow Boundaries*, the *Marginal Region*, and the *Steam Condensate on the Margins* (Figure 4).

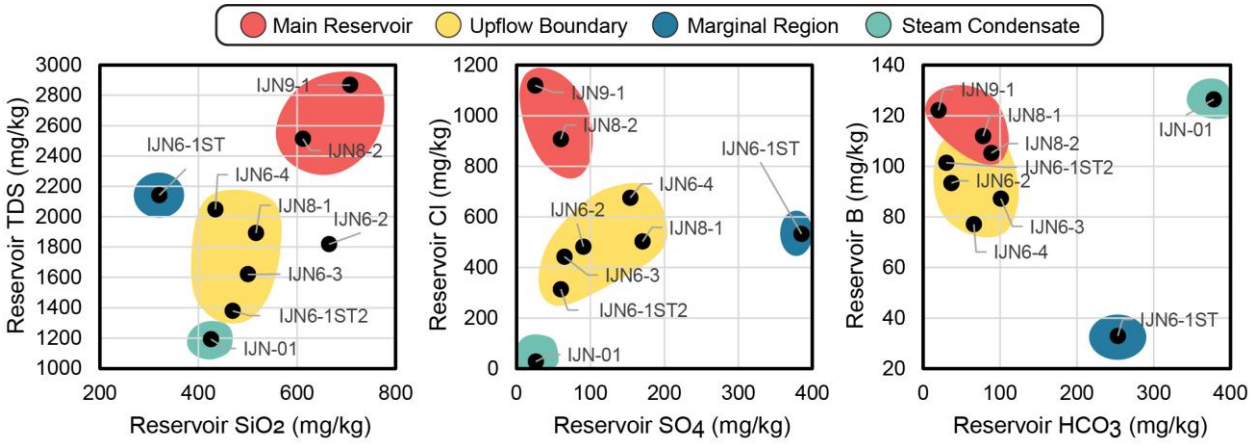


Figure 4. Bivariate plots of chemistry for calculated reservoir compositions at Ijen (calculations made using WATCH; Arnórsson et al., 1982).

The *Main Reservoir* group constitutes the upflow chemistry at Ijen, as encountered by IJN9-1, IJN8-2, and IJN6-2 (the latter being transitional from this group to the *Upflow Boundary* group). This *Main Reservoir* group is a neutral pH, Na-Cl fluid, with ~0.25-0.3 wt% TDS, ~0.15-0.3 wt% of dissolved NCGs, CO_2/H_2S molar ratios of ~15, and with the highest quartz geothermometers (284-310°C); with recognition that the reliability of T_{qtz} can sometimes be dubious at >300°C reservoir conditions. The *Upflow Boundary* group includes IJN6-1ST2, IJN6-3, IJN6-4, and IJN8-1. These wells have lower quartz and Na-K-Ca geothermometers (240-260°C) as well as lower Cl and TDS (0.14-0.21 wt%), but can have higher concentrations of HCO_3, SO_4, and NH_3 relative to the *Main Reservoir* group, suggesting the influence of some marginal recharge fluids (and perhaps some diluting steam condensate in some cases, e.g., IJN6-1ST2 and IJN6-3).

The *Marginal Region* group includes IJN6-1ST and is characterized by the lowest quartz geothermometer value (216°C), the lowest B, and elevated SO_4, HCO_3, and Mg (0.4 mg/kg compared with ~0.01 mg/kg for all other well chemistries). The fluid in this group is believed to represent a reservoir fluid that is substantially mixed with marginal recharge fluids. The *Steam Condensate* group is represented by the IJN-01 slim hole. This fluid has very low Cl (39 mg/kg) and low overall TDS (0.15 wt%) but is elevated in volatile components such as B and HCO_3.

4 WELLFIELD INFORMATION

4.1 Downhole Pressure and Temperature

Wells at Ijen take an anomalously long time to heat to equilibrium conditions; a phenomenon dominantly attributed to the low background permeability characteristics of the reservoir. The majority of wells at Ijen show continued heating after 6 months (Figure 5).

The interpretation of static formation pressure and temperature conditions for wells at Ijen requires the separation of effects related to intrawellbore (e.g., crossflow, convection, and steam/gas caps) and transient (e.g., heat-up) processes that perturb the measured data from equilibrium formation conditions. P-T profiles displayed in Figure 6 are interpretations of natural state formation conditions without these complications. When these temperatures are interpreted in 3D, isotherms reveal the existence of 320-350°C quasi-isothermal conditions in the subsurface regions intersected by IJN9-1, 8-2, and 6-1ST2 (Figures 2A and 8). The broad isotherm geometry is elongated WNW-ESE, with very steep lateral temperature gradients occurring to the southwest where a ~175°C temperature drop occurs over a lateral distance of 1000 m from IJN6-1ST2 to IJN5-1.

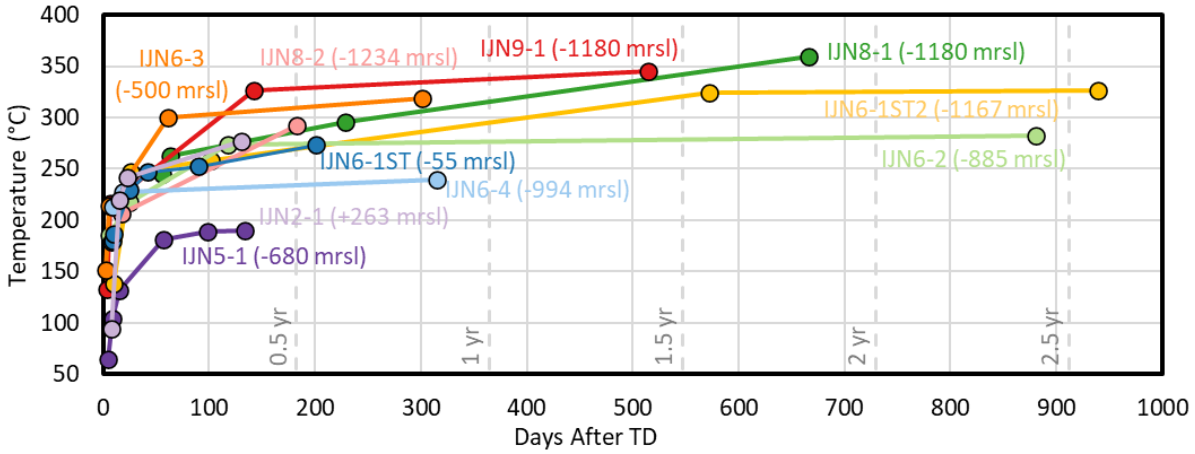


Figure 5. Static temperature heat-up trends for select elevations in Ijen wells. Elevations of data have been chosen to minimize intrawellbore effects that could otherwise mask the broad heat-up trend.

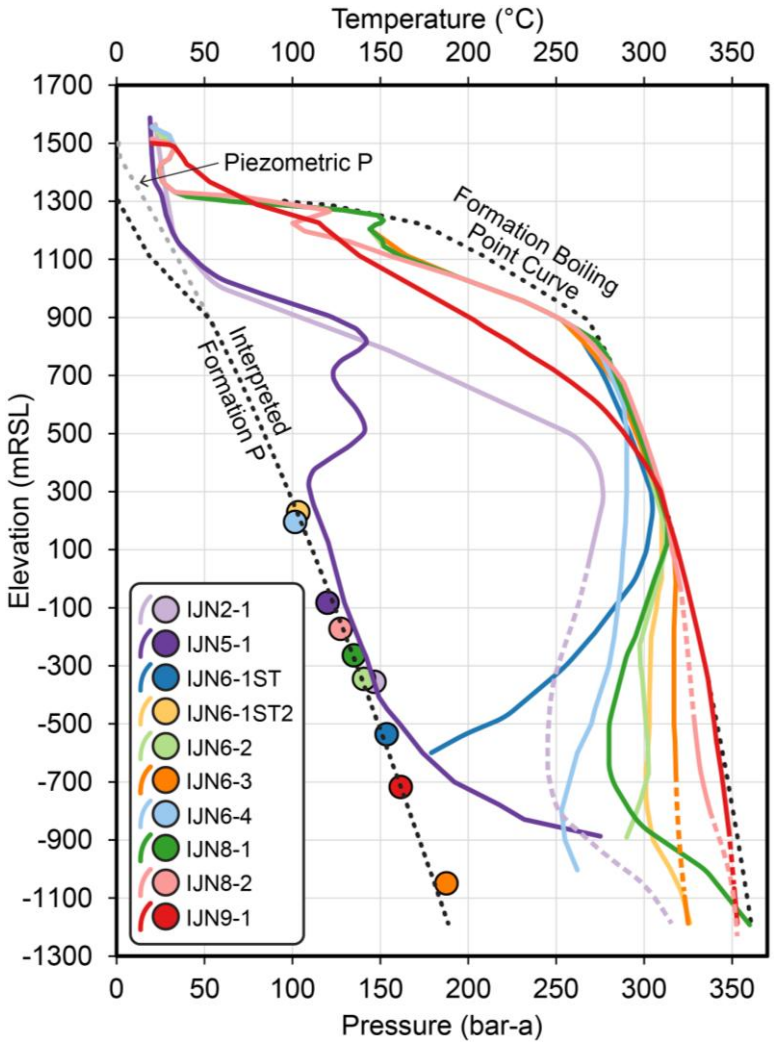


Figure 6. Interpreted natural state formation P-T. A P gradient >hydrostatic occurs within the elevation range of the inferred aquiclude (from +900 to +1100 mRSL). Dash T profiles = elevated uncertainty.

Boiling point conditions within the reservoir are detected in the wells as shallow as +750 mRSL, roughly at 825 mVD beneath the central regions of the production field. Boiling extends down to elevations of +200 mRSL in the majority of production wells in the field. IJN9-1 is interpreted to have natural state boiling point conditions extending to a deeper elevation of -450 mRSL, consistent with a location closest to the deep upflow.

Pressure control points (pivot points) for all wells drilled in the reservoir to-date align to provide a piezometric level at approximately +1450 mRSL. The expected elevation of the water table in the vicinity of the field is approximately +1300 mRSL (~275 mVD beneath the average surface elevation of the wellfield), suggesting an approximate reservoir overpressure of ~15 bar. The elevation of the confining aquitard containing this overpressure is approximated to +900 to +1100 mRSL; a region that is characterized by abundant smectite alteration within the lower section of the hydrothermal clay cap (argillic alteration zone) of the system.

A 75 m-thick shallow ~150°C outflow following the boiling point curve occurs at the water table, which is believed to represent a hot aquifer within the Genteng Unit volcanics above the inferred elevation of the aquitard. A shallower ~40°C warm (steam-heated?) perched aquifer occurs at ~1500 mRSL. A deeper >500 m-thick south-/southeast-directed outflow with an average elevation of +300 mRSL is interpreted from the temperature inversion of IJN2-1, and to a lesser extent, IJN6-2.

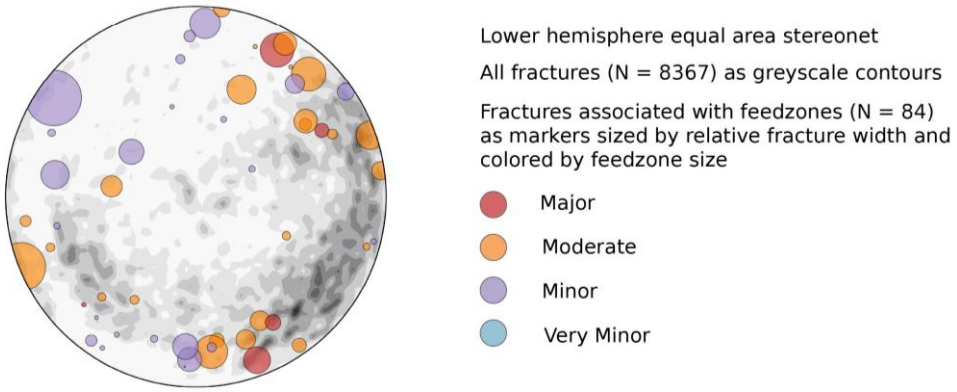


Figure 7. Feedzone fractures (plotted as poles to planes) compared to all fractures imaged.

4.2 Well Permeability and Flow Characteristics

Permeability at Ijen is related to distributed fracture networks, where strike-trends of fractures that correspond with moderate and major feedzones are often relatable to the NE-, WNW-, and NW-striking fault trends discussed in Section 2.2 (Figure 7). Each well has between 5 to 9 feedzones that contribute to production (or injection). Productivity indices for the wellfield are universally low, ranging from 0.26 to 0.66 kg/s/bar (based on calibrated wellbore models; Table 1).

Wells at Ijen flow with a wide range of excess enthalpy that varies as a result of two interacting processes: (1) preferential migration of steam from feedzone fractures in the two-phase region from +750 to +200 mRSL, and/or (2) flashing in the formation due to near-wellbore pressure drawdown, a phenomenon that is pronounced in the Ijen geothermal system owing to the low bulk permeability of the reservoir rock. Excess enthalpy contributions for individual wells at Ijen range from 0 kJ/kg in IJN9-1 to >1000 kJ/kg in IJN6-1ST2.

Table 1. Well permeability and flow characteristics at Ijen. I.I.s and P.I.s from wellbore models. Flow metrics from tracer flow test (TFT) data and assumptions of 20 barg WHP. Blue values are expected to be underestimations (IJN8-1 was still on a heating trend when the TFTs were collected).

Well	Use*	GL Elev mrsl	Total Depth mMD_{KB}	Casing Depth mMD_{KB}	I.I. kg/s/bar	P.I. kg/s/bar	Flow. WHP barg	Total Flow kg/s	Steam Flow kg/s	Brine Flow kg/s	H kJ/kg	Inj Cap** kg/s	Inj Cap*** kg/s
IJN2-1	Idle/ Inj	1565	3041	1186	1.73	-	-	-	-	-	-	65	95
IJN5-1	Inj	1588	2700	1239	2.93	-	-	-	-	-	-	113	158
IJN6-1ST	P&A	1598	2300	1296	1.78	0.9	-	-	-	-	-	-	-
IJN6-1ST2	Prod	1557	2770	505	2.29	0.56	20	36.2	21.2	15.0	1986	-	-
IJN6-2	Prod	1557	2644	630	2.17	0.52	20	27.0	10.5	16.5	1600	-	-
IJN6-3	Prod	1557	2905	693	3.25	0.66	20	34.0	13.1	20.9	1596	-	-
IJN6-4	Prod	1557	2615	645	3.82	0.64	20	23.8	12.2	11.6	1842	-	-
IJN8-1	Idle/ Prod	1515	2800	690	2.26	0.46	20	11.0	3.1	7.9	1400	-	-
IJN8-2	Prod	1515	2820	682	1.98	0.61	20	32.2	10.4	21.8	1474	-	-
IJN9-1	Idle/ Prod	1500	2723	1200	2.08	0.26	20	29.	9	20.0	1450	-	-

*Well use as of Q4 2025 | **Injection capacity at 0 WHP | ***Injection capacity at 17 barg WHP

5 INTEGRATED CONCEPTUAL MODEL

5.1 Reservoir Temperatures, Pressures, and Hydrology

Upflow at Ijen manifests as a NNE-dipping, WNW-elongated, 300-350°C hydrothermal plume that appears to be influenced by dilated WNW-striking structures such as the Pandean and Geleman Faults.

There are three vertically distinct outflows branching out from the upflow at Ijen. From deepest to shallowest these are: (1) A deeper, >500 m-thick, SE-directed outflow at an average elevation of +300 mRSL, likely following the structural grain of the Pandean and Geleman Faults towards IJN2-1; (2) A tiered set of two outflow lobes channelized to the southwest along volcanostratigraphic horizons at the base of the clay cap (+900 mRSL); (3) a thin, shallow, NE-directed <150°C outflow occurring at and just below the water table above the pressure containment aquitard within the clay cap.

There are no active thermal manifestations that can be confidently associated with the Ijen geothermal system, nor are there expressions of fossil thermal manifestation activity at the field. The Blawan warm springs occur 7 km to the north, near the northern rim of the caldera, with a mixed chemistry that cannot be definitively linked to the Ijen geothermal system. The updated model of the Ijen geothermal system also validates its geologic disconnection from the hyperacidic lake and superheated fumaroles of the Kawah Ijen vapor core system, which occur at elevations of ~2150 mRSL, 8 km to the east of the Ijen geothermal system on the NW flank of Mt. Merapi.

The lack of surface thermal manifestations near the Ijen field area can be explained by some or all of the following four system characteristics: (1) A competent hydrothermal clay cap (which contains 15 bar of overpressure in the deeper reservoir), (2) layered shallow aquifers, including one at the water table that sweeps heat from above the aquitard of the system at approximately +1300 mRSL and shallower perched meteoric aquifers at +1500 mRSL that further sweep any leaked heat or gas, (3) a relatively deep (~275 mVD) water table, and (4) competent and relatively unfractured capping volcanic sequences prone to forming interlayered aquifers and aquicludes.

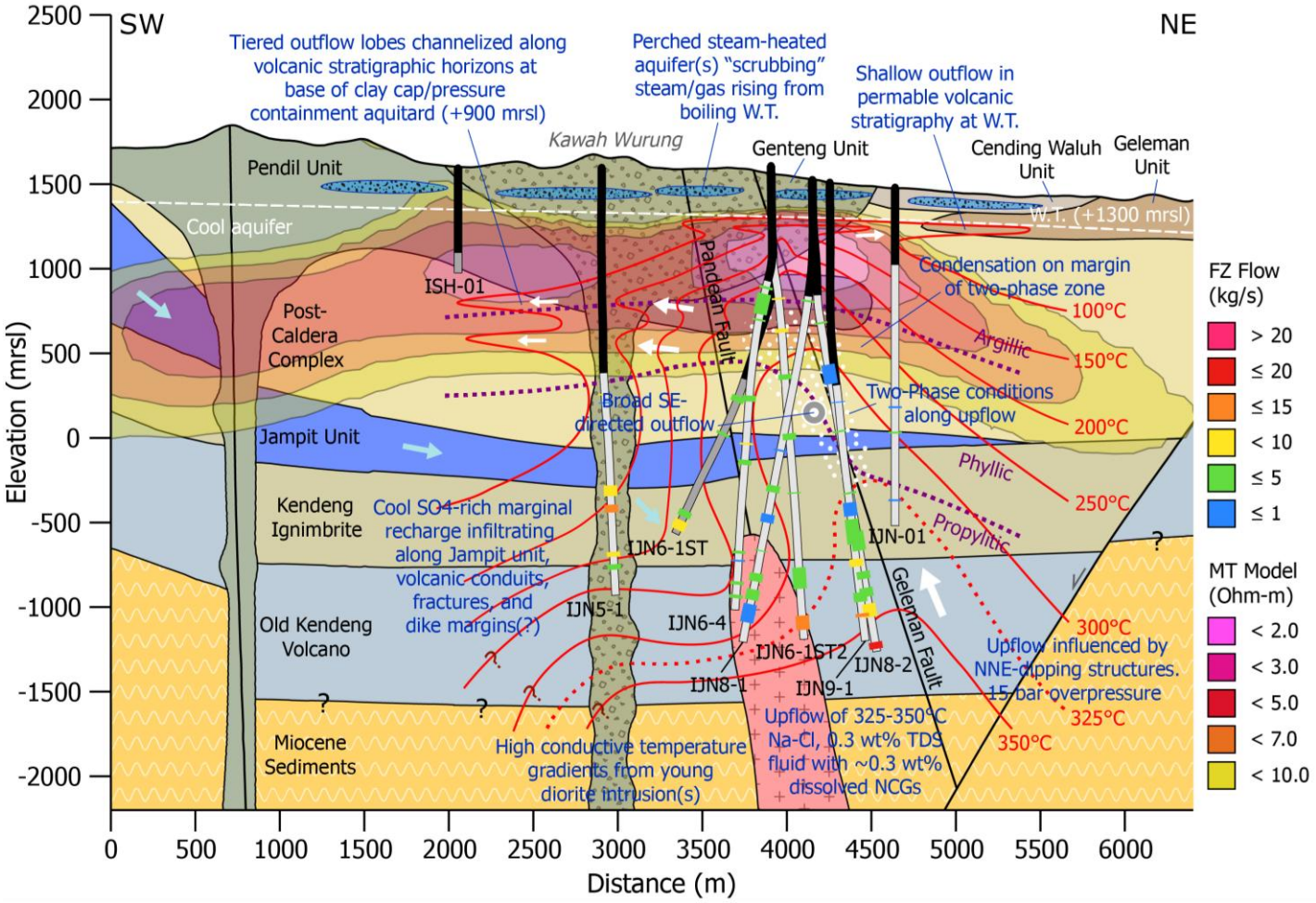


Figure 8. Conceptual model cross-section through the Ijen geothermal system. FZ Flow refers to potential feedzone production/injection flow based on data derived from long-term flow and injection testing. Cross-section location is displayed on Figure 2A.

5.2 Reservoir Chemistry

The deep upflow fluid at Ijen is a neutral pH, Na-Cl, ~0.3 wt% TDS fluid with ~0.15-0.3 wt% dissolved NCGs, with cation and silica geothermometers agreeing with the >300°C conditions of the upflow. There are steep chemical gradients with distance away from the central upflow region intersected by IJN9-1 and IJN8-2. These gradients represent the increasing influence of SO_4 and HCO_3-enriched marginal fluids and potentially steam condensates with distance from the core of the upflow. Steep chemical gradients over a small distance at Ijen are another manifestation of the low bulk permeability of the system.

5.3 Permeability Characteristics and Structural Context

A left-step between the regional-scale sinistral strike-slip Gumitir and Ringghi-Baluran faults is expected to create a domain of localized relative transtension/extension in the southern region of the Kendeng Caldera, facilitating permeability for geothermal fluid circulation as well as magma ascent related to the abundant Quaternary intracaldera monogenetic volcanism in the vicinity. The WNW elongation of upflow at Ijen is interpreted as being influenced by the Geleman and Pandean Faults. The orientation of these faults is expected to be inherited from basement structures of the East Java-West Sulawesi block. Feedzones at Ijen relate to distributed fracture networks, with inferred feedzone-related fractures following the NE-, NNE-, WNW-, and NW-striking fault trends identified in the region.

5.4 Host Rock

The host rock for the Ijen geothermal system is predominantly andesitic lavas and pyroclastics from pre-, syn-, and post-Kendeng Caldera volcanism. Basement carbonate-rich Miocene sediments are expected to occur within 500 mVD below the deepest wells drilled to-date at Ijen, at elevations of approximately -1500 to -1600 mRSL.

5.5 Resource Area and Thickness

The area of the Ijen resource, when defined as the area of the mean production temperature isotherm (~285°C) at a slice that is halfway through the thickness, is assessed to be 1.25 to 1.75 km^2 (80% confidence interval with a mean of 1.5 km^2. The largest uncertainty of this area is on the southeastern margin (i.e., the region between IJN6-2 and IJN2-1), where there is an absence of subsurface data.

The southwestern margin of the system is primarily defined by the observed temperature inversions in IJN6-1ST and IJN5-1. These were the first full-size wells drilled in the exploration campaign and were initially targeting upflow based on promising indications from the 3D MT model. The temperature pattern observed from the very slow heat-ups significantly modified the conceptual model and reduced the estimated project area and capacity. The northern margin of the resource is marked by deepening alteration zone boundaries; imaged as a deepening conductor in the 3D MT inversion model. The likely maximum western extent to the reservoir is also suggested by the abrupt termination of the <5 ohm-m conductor 900 m to the west of IJN9-1.

The thickness parameter of the resource has been defined here as the vertical depth from the top of the average reservoir isotherm (285°C) to the base of interpreted sweep of heat from the injection to the production wells. A density-driven 500 m downflow of injection water is interpreted from the base of the deepest injection feedzone, providing the base elevation for this approximate heat-sweeping thickness. Following this logic, the thickness of the resource at Ijen is approximately 2000 m (1750-2250 m 80% confidence interval). The maximum depth of circulation beneath the Kawah Wurung region may also be dictated by silica self-sealing, as quartz solubility in pure water becomes retrograde beyond temperatures of ~340°C (Fournier, 2007).

5.6 Heat Source

The heat source for the Ijen geothermal system is expected to be mid- to upper-crustal magmatic bodies that are expected to reside beneath the southern half of the Kendeng Caldera. Manifestations of this young magmatism include the microdiorite intersected in the deep sections of IJN6-4 and IJN8-1, the very high conductive temperature gradient near this intrusion, and the highest recorded temperature in the field of 359°C at the TD of IJN8-1 within the microdiorite intrusion.

5.7 Pre-Production System Evolution

The existence of alteration mineral assemblages with expected stability temperatures that are higher than the measured temperatures in some parts of the reservoir and lower in others, indicate that both the cold water hydrology and the heat flux in the system have changed over a short time, geologically. The occurrence of elevated smectite concentrations in subsurface regions below Pad 6 where the temperatures are currently 250-

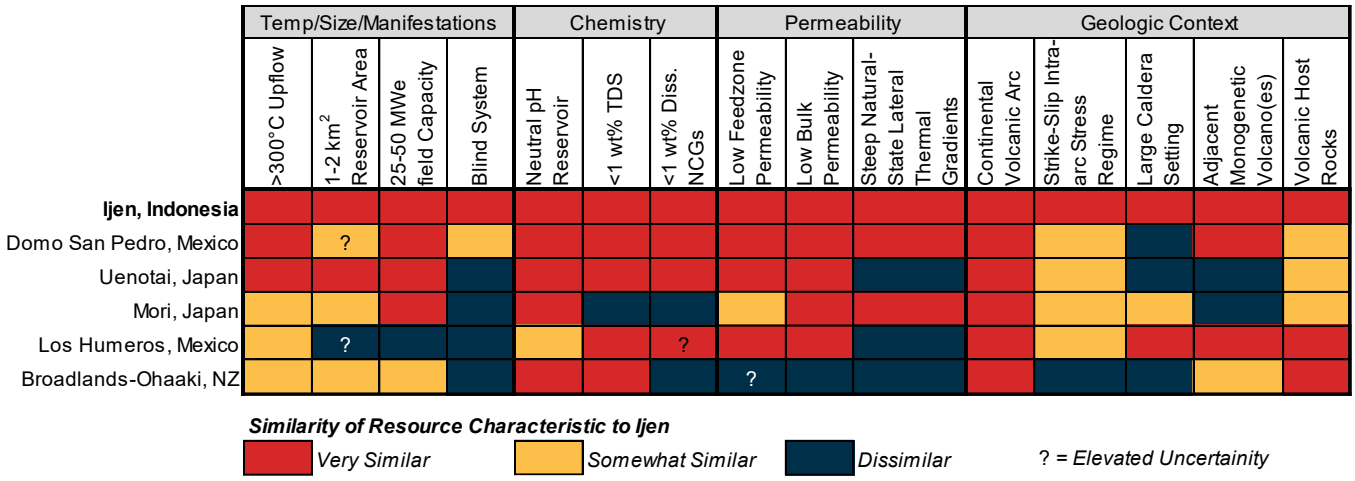
280°C, far above the inferred upper-limit of 220°C for the transition of mixed-layer illite-smectite to end-member illite, suggests that a geologically-recent heating event has occurred in this part of the reservoir. Conversely, the occurrence of a propyllitic mineral assemblage, with some resorbed epidote textures, in sections of IJN5-1 where subsurface temperatures are currently 125-175°C, suggests a pronounced cooling evolution of this southwest region of the field.

The steep lateral temperature and chemical gradients to the southwest of the field, the high temperature gradients at the base of IJN8-1 in association with microdiorite, and the partial "hole" in the <2 ohm-m conductor in the center of the Kawah Wurung crater, suggest that geologically-recent dike intrusions beneath the Kawah Wurung crater and potentially related diatreme-forming volcanic events may have resulted in a change of the hydrology of the system. Permeability along dike margins and/or diatreme may have facilitated flow of cooler meteoric recharge fluids in the southwest regions of the field. Pronounced heat input from this same intrusive activity may have invigorated the pronounced >325°C upflow that is intersected by IJN9-1, IJN8-2, and the shallow sections of the Pad 6 wells. In essence, the interpretation is that the intrusive activity has resulted in both heating of the northeast and central reservoir and cooling of the southwest reservoir margin.

5.8 Key Conceptual Model Uncertainties

The long heat-up times (>6 months and sometimes >1 year) for wells at Ijen results in transient effects in the measured data that complicate the interpretation of equilibrium formation P-T profiles. Additionally, intrawellbore effects such as crossflow, convection around liner tops, wellbore steam/gas cap formation, and downward crossflow of steam cap condensate also serve to complicate the interpretation of the measured static P-T data. As a result, although the overall geometry and scale of the reservoir elements are reasonably well resolved for a field at this stage of development, the details of the natural state isotherm model for the system remains locally uncertain. Interpreted formation P-T profiles for wells with 6 months or less of static heat-up surveys, and that show signs of continued heating (namely, IJN8-2 and IJN2-1) have a higher degree of uncertainty than other wells in the field. Deep temperature inversions in the measured P-T data of IJN6-3, IJN8-2, and IJN9-1 below elevations of approximately -700 mrsl are interpreted as non-equilibrium, transient heat-up effects; however, there remains the possibility that these features are in-fact representative of equilibrium conditions and reflect geologically-recent deep cool water incursions into the system. These intervals of elevated interpretation uncertainty are depicted with dashed lines in the interpreted temperature profiles provided in Figure 6. Additionally, there remains an elevated degree of uncertainty in the structural model for Ijen and the relationship of specific reservoir-scale faults to the documented feedzones.

Table 2. Field analog comparison table.



5.9 Analogs

As conceptual models were developed for Ijen, analogs were used to constrain the likelihood of specific model elements. Several developed high temperature/low permeability fields in the continental arcs of Mexico and Hokkaido and northern Honshu in Japan serve as reasonable, albeit imperfect, analogs for the Ijen geothermal system (Table 2). The 35.5 MW Domo San Pedro field in the western region of the Trans-Mexican Volcanic Belt shares notable reservoir and geologic similarities with Ijen, and surface manifestations at this analog field are limited to distal warm springs (Orozco et al., 2019; Rodriguez et al., 2019). While not a blind system, the 29 MW Uenotai geothermal field in Japan has permeability, temperature, chemistry, area, and geology (Menzies et al., 1990; Butler et al., 2004) that can be usefully compared to Ijen. Because of its caldera setting and recent small

volcanic vents, the 25 MW Mori geothermal field in Japan had been used as an analog for Ijen prior to drilling, and the steep thermal gradients and hydrology influenced by a funnel-like volcanic conduit proved to be an apt analog; however, other properties like the higher TDS and gas concentrations at Mori (Yoshida, 1991; Hanano et al., 2005) are not analogous to the Ijen reservoir fluid. The 94 MW Los Humeros geothermal field in Mexico is hosted in a large caldera setting, similar to Ijen, and it has some permeability, temperature, and geologic characteristics that make attributes of it analogous to some resource parameters at Ijen (Sánchez-V. & Torres-Rodriguez, 1994). However, the area and capacity of Los Humeros is likely larger than that of Ijen, and the low pH deep reservoir conditions at Los Humeros (Izquierdo et al., 2011) are not analogous to conditions currently detected at Ijen. Additionally, Broadlands-Ohaaki, New Zealand is a higher permeability system than Ijen, but has some similarities, including area, capacity, and young volcanic conduits providing a pathway for the conveyance of shallow fluids into the deeper reservoir, e.g., the buried Ohaaki Rhyolite dome. A notable distinction is that the downflow at Ohaaki is likely the result of production-induced pressure drawdown and not a natural state phenomenon (Rissmann et al., 2011; Mroczek et al., 2016), like it is at Ijen. Analog system knowledge has helped guide the conceptual model development, well targeting, and development strategy for Ijen, and such analogs continue to provide insight to guide operational strategies.

6 CONCLUSIONS

Ijen represents a high temperature geothermal system with characteristics that set it apart from other currently developed geothermal fields in Indonesia, namely: it is devoid of conspicuously-linked surface manifestations, it is characterized by low permeability conditions, its very hot upflow is small in aerial extent with steep thermal and chemical boundaries away from its center, and the hydrothermal mineralogy suggests temperatures that are both hotter and colder than the present reservoir conditions in different parts of the field. These resource characteristics presented unique challenges for data interpretation and strategy development. For example, the very slow temperature equilibration times and the observed disequilibrium mineralogy increased decision uncertainty during the drilling campaigns. The implementation of a conceptual model-driven approach during the exploration and development of Ijen was critical for achieving the project's realized success.

Acknowledgements

The authors would like to thank all parties involved in the exploration and development of the Ijen geothermal resource. A special thanks to the joint-venture, P.T. Medco Cahaya Geothermal, plus the two parent shareholders, Ormat Technologies Inc. and P.T. Medco Power Indonesia for the permission to publish on these data. Special thanks to Eka Satria and Bob Sullivan for making this joint-venture happen and for supporting science-based decision-making along the way.

REFERENCES

Arnórsson, S., Sigurdsson, S., & Svavarsson, H. (1982). The chemistry of geothermal waters in Iceland. I. Calculation of aqueous speciation from 0° to 370°C. Geochimica et Cosmochimica Acta, 46(9), 1513–1532.

Bird, D. K., Schiffman, P., Elders, W. A., Williams, A. E., & McDowell, S. D. (1984). Calc-silicate mineralization in active geothermal systems. Economic Geology, 79(4), 671–695.

Browne, P. (1984). Lectures on geothermal geology and petrology. United Nations University Geothermal Training Programme, 90 p.

Butler, S. J., Sanyal, S. K., Klein, C. W., Iwata, S., & Itoh, M. (2004). Numerical simulation and performance evaluation of the Uenotai geothermal field, Akita Prefecture. GRC Transactions, 28, 455–460.

Caudron, C., Syahbana, D. K., Lecocq, T., Van Hinsberg, V., McCausland, W., Triantafyllou, A., Camelbeeck, T., Bernard, A., & Surono. (2015). Kawah Ijen volcanic activity: A review. Bulletin of Volcanology, 77(3), 16 p.

Dermawan, F., Webbison, S., Johnson, A., Libbey, R., Marini, L., Mroczek, E., Saputra, I., Utomo, D., Abiyudo, R., & Murphy, J. (2025). Natural state chemistry of the Ijen geothermal field – a blind geothermal system. Proc. 47th New Zealand Geothermal Workshop, 10 p.

Ekström, G., Nettles, M., & Dziewoński, A. M. (2012). The global CMT project 2004–2010: Centroid-moment tensors for 13,017 earthquakes. Physics of the Earth and Planetary Interiors, 200–201, 9 p.

Ferrill, D. A., Smart, K. J., & Morris, A. P. (2020). Fault failure modes, deformation mechanisms, dilation tendency, slip tendency, and conduits v. seals. Geological Society, London, Special Publications, 496(1), 75–98.

Fournier, R. O. (2007). Hydrothermal systems and volcano geochemistry. In D. Dzurisin, Volcano Deformation (pp. 323–341). Springer Berlin Heidelberg.

Gunderson, R., Cumming, W., Astra, D., & Harvey, C. (2000). Analysis of smectite clays in geothermal drill cuttings by the methylene blue method: For well site geothermometry and resistivity sounding correlation. Proc. World Geothermal Congress, 1175–1181.

Hall, R. (2002). Cenozoic geological and plate tectonic evolution of SE Asia and the SW Pacific: Computer-based reconstructions, model and animations. Journal of Asian Earth Sciences, 20(4), 353–431.

Hall, R., Clements, B., & Smyth, H. R. (2009). Sundaland: Basement character, structure and plate tectonic development. Proc. Indonesian Petroleum Association, 27 p.

Hall, R. (2011). Australia–SE Asia collision: Plate tectonics and crustal flow. Geological Society, London, Special Publications, 355(1), 75–109.

Hall, R. (2012). Late Jurassic–Cenozoic reconstructions of the Indonesian region and the Indian Ocean. Tectonophysics, 570–571, 41 p.

Hanano, M., Kajiwara, T., Hishi, Y., Arai, F., Asanuma, M., Sato, K., & Takanohashi, M. (2005). Overview of Production at the Mori Geothermal Field, Japan. Proc. World Geothermal Congress, 10 p.

Handley, H. K., Macpherson, C. G., Davidson, J. P., Berlo, K., & Lowry, D. (2007). Constraining fluid and sediment contributions to subduction-related magmatism in Indonesia: Ijen volcanic complex. Journal of Petrology, 48(6), 1155–1183.

Izquierdo, G., Aragón, A., & Díaz, D. (2011). Evidence of deep acid fluids in the Los Humeros geothermal system, Mexico. GRC Transactions, 625–630.

Marliyani, G. I., Helmi, H., Arrowsmith, J. R., & Clarke, A. (2020). Volcano morphology as an indicator of stress orientation in the Java Volcanic Arc, Indonesia. Journal of Volcanology and Geothermal Research, 400, 19 p.

Menzies, A. J., Antunez, E. U., Sanyal, S. K., Naka, T., Takeuchi, R., Iwata, S., Saeki, Y., & Inoue, T. (1990). A case history of a multi-well interference test program at the Uenotai geothermal field, Akita prefecture, Japan. GRC Transactions, 1241–1248.

Mroczek, E. K., Milicich, S. D., Bixley, P. F., Sepulveda, F., Bertrand, E. A., Soengkono, S., & Rae, A. J. (2016). Ohaaki geothermal system: Refinement of a conceptual reservoir model. Geothermics, 59, 311–324.

Orozco, V. M. R., Tapia, D. A., Tirado, J. G., Pineda, E. R., & Aguilar, F. O. (2019). Preliminary Conceptual Model of the Domo San Pedro Geothermal Field—Western Sector of Trans-Mexican Volcanic Belt, Nayarit, Mexico. Proc. 44th Workshop on Geothermal Reservoir Engineering, 8 p.

Ramos, S. G. (2002). Potential constraints to the development of the Rangas sector based on petrologic evaluation of the Bacman geothermal field, Philippines. Proc. Twenty-Seventh Workshop on Geothermal Reservoir Engineering, 9 p.

Rissmann, C., Nicol, A., Cole, J., Kennedy, B., Fairley, J., Christenson, B., Leybourne, M., Milicich, S., Ring, U., & Gravley, D. (2011). Fluid flow associated with silicic lava domes and faults, Ohaaki hydrothermal field, New Zealand. Journal of Volcanology and Geothermal Research, 204(1–4), 12–26.

Rodriguez, E., Ocampo, F., Reyes, V., Avalos, D., & Garcia, J. (2019). Preliminary Geochemical Model of the Domo San Pedro Geothermal Field in San Pedro Lagunillas, Mexico. Stanford University, 15 p.

Sánchez-V., R., & Torres-Rodriguez, M. A. (1994). Well behaviour in the Los Humeros geothermal field. GRC Transactions, 18, 283–290.

Scher, S., Williams-Jones, A. E., & Williams-Jones, G. (2013). Fumarolic activity, acid-sulfate alteration, and high sulfidation epithermal precious metal mineralization in the crater of Kawah Ijen volcano, Java, Indonesia. Economic Geology, 108(5), 1099–1118.

Siler, D. L. (2023). Structural discontinuities and their control on hydrothermal systems in the Great Basin, USA. Geoenergy, 1(1), 10 p.

Sitorus, K. (1990). Volcanic stratigraphy and geochemistry of the Idjen Caldera Complex, East Java, Indonesia. MSc thesis, University of Wellington, New Zealand.

Sujanto, Syarifuddin, M. Z., & Sitorus, K. (1988). Geological Map of the Ijen Caldera Complex, East Java. Direktorat Vulkanologi.

Yoshida, Y. (1991). Geochemistry of the Nigorikawa geothermal system, southwest Hokkaido, Japan. Geocehmical Journal, 25, 203–222.